Editors' Suggestion

Anomalous doping evolution of collective charge excitations in an n-type cuprate

Ke-Jun Xu,[1,2] Nathan Giles-Donovan,[1,2] Stefano Agrestini,[3] Jaewon Choi,[3,*] Mirian Garcia-Fernandez,[3] Kejin Zhou,[3,†] Junfeng He,[4,5,‡] Costel R. Rotundu,[4,5,§] Young S. Lee,[4,5,6] Thomas P. Devereaux,[4,5,7] Zhi-Xun Shen,[4,5,6,8] Dung-Hai Lee,[1,2,‖] Robert J. Birgeneau,[1,2,¶] and Wei-Sheng Lee[4,**]

[1]*Department of Physics, University of California, Berkeley, California 94720, USA*
[2]*Material Sciences Division, Lawrence Berkeley National Laboratory, Berkeley, California 94720, USA*
[3]*Diamond Light Source, Harwell Campus, Didcot, Oxfordshire OX11 0DE, United Kingdom*
[4]*Stanford Institute for Materials and Energy Sciences, SLAC National Accelerator Laboratory, 2575 Sand Hill Road, Menlo Park, California 94025, USA*
[5]*Geballe Laboratory for Advanced Materials, Stanford University, Stanford, California 94305, USA*
[6]*Department of Applied Physics, Stanford University, Stanford, California 94305, USA*
[7]*Department of Materials Science and Engineering, Stanford University, Stanford, California 94305, USA*
[8]*Department of Physics, Stanford University, Stanford, California 94305, USA*

(Received 20 May 2026; accepted 14 October 2026; published 3 November 2026)

Metallic systems with delocalized valence electrons host collective charge density oscillations known as plasmons. On the other hand, conventional insulators do not have free electrons and the low-energy charge degrees of freedom are pinned to the ions. The fate of the collective charge excitations in the intermediate regime is an outstanding question. This problem is especially important for strongly correlated systems such as the layered cuprates, where unconventional superconductivity and other emergent phenomena arise from valence electrons on the border between Mott localization and itinerancy. Using resonant inelastic xray scattering, we track this evolution in the prototypical electron-doped cuprate $Nd_{2-x}Ce_xCuO_4$. We find a continuous transformation of the low-energy charge response: from an acoustic plasmon in the metallic regime, to a gapped mode with a dispersion anomaly at intermediate doping, and finally to a nearly dispersionless 139 meV excitation at half filling. The 139 meV excitation at zero doping has approximately twice the energy of the oxygen phonons responsible for the dispersion anomaly observed in angle-resolved photoemission spectroscopy. To explain this evolution, we introduce an

[*]Present address: Department of Physics and Astronomy, Seoul National University, Seoul 08826, Republic of Korea.
[†]Present address: National Synchrotron Radiation Laboratory and School of Nuclear Science and Technology, University of Science and Technology of China, Hefei 230026, China.
[‡]Present address: Department of Physics, University of Science and Technology of China, Hefei 230026, China.
[§]Present address: Charlotte, North Carolina, USA.
[‖]Contact author: dunghai@berkeley.edu
[¶]Contact author: robertjb@berkeley.edu
[**]Contact author: leews@stanford.edu

Published by the American Physical Society under the terms of the Creative Commons Attribution 4.0 International license. Further distribution of this work must maintain attribution to the author(s) and the published article's title, journal citation, and DOI.

inhomogeneous microscopic framework where plasmons in metallic regions couple with two-phonon excitations in insulating regions. These results establish a unified picture of collective charge excitations across the phase diagram of electron-doped cuprates and reveal a missing link in the charge dynamics of carrier doped Mott insulators.

DOI: 10.1103/nbry-mk8w

I. INTRODUCTION

While plasmons in good metals are well understood [1], recently there has been strong interest in the behavior of collective charge excitations in strongly correlated systems on the border between itinerancy and localization. This is because many puzzling phenomena such as strange metals [2–5] and high-temperature superconductivity [6,7] manifest in the charge sector upon doping the Mott insulating state [8–10]. The cuprates is an ideal model platform for investigating unconventional charge dynamics, as they host a rich phase diagram of insulating, metallic, and superconducting states [7]. At half filling, the strong Coulomb potential localizes charge carriers to a single electron per site, leading to a Mott-insulating ground state. When heavily doped, these compounds behave like metals with Fermi-liquid-like properties [11,12]. In the intermediate doping regime, there are signatures of a strange metal phase [2–5], where the charge quasiparticle is not well defined [13]. A pressing question is how the collective charge excitations behave, if they exist at all, in the underdoped regime and across the Mott transition.

Previous resonant inelastic x-ray scattering (RIXS) measurements at the Cu L edge observed sharp acoustic plasmons in electron-doped cuprates near optimal doping [14]. The plasmon dispersion appears to be gapless at the Brillouin zone center for nonzero perpendicular wave vectors, consistent with a two-dimensional confinement of the electrons with weak interlayer hopping. When the interlayer hopping is strong, as in the case of the infinite layer electron-doped cuprates, there can be a finite Brillouin zone center gap induced by interlayer hopping [15]. P-type plasmons have also been observed by RIXS at the O K edge [16], as the doped holes reside on the oxygen sites. The p-type plasmons tend to be weaker in intensity compared to the n-type plasmons [17].

The relationship between these plasmons and high-transition-temperature superconductivity is a long-standing question [18–20]. To gain insight into this question, it is imperative to reveal how these plasmons evolve toward the lightly doped regime, where the pairing interaction is thought to be strong [21]. The previous RIXS works on the electron-doped cuprates mainly focused on $La_{2-x}Ce_xCuO_4$ films [22], which tend to be metallic even in the nominally underdoped regime. They also cannot be synthesized as a single phase for doping below about 10% [23], thus limiting the accessible doping range. A previous work studied the doping dependence of plasmons in hole-doped $La_{2-p}Sr_pCuO_4$ and apparently found a reduction of the plasmon energy with decreasing doping down to $p = 0.05$ [24]. However, the broadness of the p-type plasmons and limited momenta points prevented an accurate extraction of the plasmon dispersions.

In this work, we investigate the behavior of collective charge excitations in a prototypical electron-doped cuprate $Nd_{2-x}Ce_xCuO_4$ from $x = 0$ to $x = 0.14$ using RIXS at the Cu L_3 edge. This doping range spans a large region of the phase diagram from the Mott-insulating parent compound to near the optimally doped superconducting regime [25–27]. The lightly doped regime in electron-doped cuprates is of particular interest, as recent angle-resolved photoemission spectroscopy (ARPES) studies found a hierarchy of energy gaps strongly affecting the low-energy valence electronic states [28]: an antiferromagnetic gap that reconstructs the Fermi surface to small pockets centered at the $(0, \pi)$ and equivalent points; an anomalous normal state gap that further gaps the reconstructed pockets. This cascade of energy gaps may strongly affect the low-energy charge dynamics in the lightly doped regime. Our current work tracks the evolution of the collective charge excitation from the Mott insulator to the superconducting regime, revealing its transformation from

a nearly dispersionless two-phonon-like mode into an acoustic plasmon through an intermediate gapped mode with a dispersion anomaly.

II. COLLECTIVE CHARGE EXCITATIONS ACROSS THE MOTT TRANSITION

We first examine the overall behavior of the low-energy collective charge excitations as a function of doping. Figure 1(a) shows energy-momentum spectra along the (h, 0, 1) direction in reciprocal space, taken with a photon energy at the peak of the Cu L_3-edge resonance (see Fig. S1 of the Supplemental Material [29]). We use σ-polarized photons (E field within the CuO plane) to highlight the charge excitation more prominently. For $x = 0.14$, we observe dispersive acoustic plasmons, similar to those reported in previous RIXS studies [14]. With decreasing electron doping, the dispersion velocity decreases, accompanied by the development of an excitation gap near the Brillouin zone center [Fig. 1(a)]. At $x = 0$, in addition to a strong magnon dispersion due to the long-range antiferromagnetic order [30], there is a collective mode at around 139 meV with no observable dispersion.

To gain further insight, we first extract an approximate dispersion velocity by linear fits at different dopings [Fig. 1(b)]. Overall, we find that the plasmon velocity does not follow the expected $\sqrt{x}$ dependence [31] at $l = 1$ for $x > 0.12$. The velocity exhibits a jump near $x = 0.12$ [Fig. 1(c)], which is associated with the antiferromagnetic Fermi surface reconstruction [32,33], where the large Fermi surface is folded across the antiferromagnetic zone boundary to form small reconstructed pockets. Concomitantly, there is a change in the carrier density from being proportional to x at low dopings to being proportional to $1 - x$ at high dopings. Example data fitting is presented in Fig. S2 of the Supplemental Material [29].

To clarify the evolution of the collective charge excitation, we first examine their nature at the limit of the Mott insulator. The RIXS energy distribution curves in Fig. 2(a) reveal the evolution of the low-energy features in undoped Nd_2CuO_4 along the (h, 0, 1) direction. Apart from the elastic line, we observe a one-phonon feature at around 50 meV, a dispersing magnon feature, and an excitation near 139 meV with apparently no observable dispersion. Here, because of long-ranged antiferromagnetic order in the undoped sample, we still observe a strong magnon feature even with σ incident photons. The magnon feature is further enhanced in the spectra taken with π photons [Fig. 2(b)]. At the same time, the 50 meV phonon and the 139 meV excitation are highlighted more prominently in the spectra taken with incident photons with σ polarization. The dispersions of the magnon and the 139 meV excitation are summarized in Fig. 2(c). We also checked the dispersion of the 139 meV mode along the l direction at a fixed h value and found that there is no appreciable dispersion perpendicular to the CuO_2 planes [Fig. 2(d)]. The dependence on the incident photon polarization and the energy scale suggest a charge origin for the 139 meV mode.

With an understanding of the behavior at half filling, we now examine the evolution of the excitation spectrum upon light doping. Figure 3(a) shows the RIXS spectra from $Nd_{1.96}Ce_{0.04}CuO_4$ along the (h, 0, 1) direction, taken with incident photons of σ polarization. The signature of the nearly dispersionless mode can still be resolved near the zone center for $h < 0.06$, but it becomes less pronounced with a slightly softened energy of about 120 meV. For higher momentum, the charge excitation intersects with the magnon to form a single peak, as electron doping weakens the magnon intensity such that both excitations have similar intensities. To distinguish between these two components, we perform polarization-resolved RIXS at $h = 0.08$ [Figs. 3(b) and 3(c)]. The magnon peak at around 100 meV, which manifest prominently in the cross-polarization $\pi\sigma'$ and $\sigma\pi'$ channels, possesses a lower energy than the charge peak (around 150 meV) extracted from the parallel polarization channels ($\pi\pi'$ and $\sigma\sigma'$). Furthermore, since the RIXS spectra taken with π-polarized photons is dominated by the magnon peak [e.g., Fig. 3(b)], it can be used to constrain the magnon peak position and extract the component of charge excitations in the polarization-integrate spectra taken with σ incident polarization for $h > 0.06$ (see Fig. S3 of the Supplemental Material [29]). The extracted dispersions of the charge and magnetic excitations in $Nd_{1.96}Ce_{0.04}CuO_4$ are

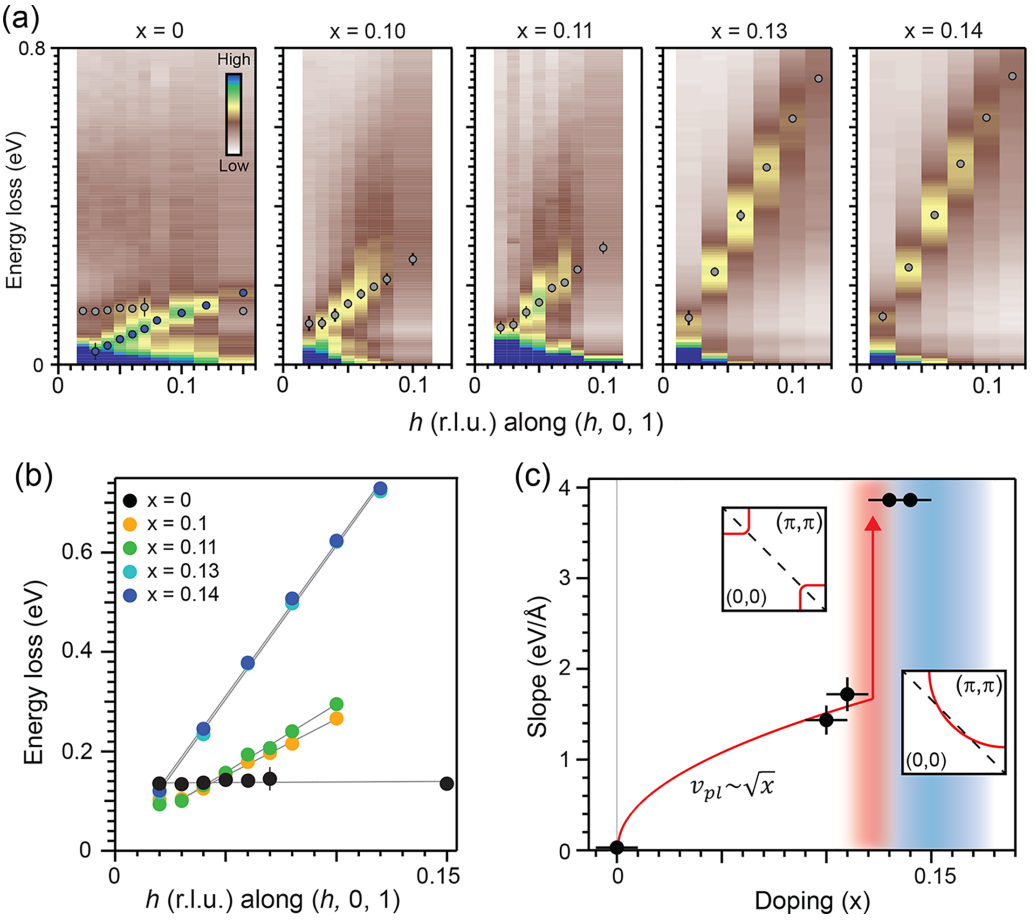


FIG. 1. Collective charge excitations in $Nd_{2-x}Ce_xCuO_4$ revealed by RIXS. (a) Color plots of energy-momentum RIXS spectra at different dopings measured with σ-polarized incident photons along the (h, 0, 1) direction. The doping levels, defined by the Ce content, are indicated above each panel. Gray dots indicate the fitted positions of the dispersive low-energy charge excitations. In the $x = 0$ sample, blue dots represent the magnon excitation and the gray dots represent the nearly dispersionless charge excitation. (b) Dispersions of the low-energy charge excitation extracted from fits of the RIXS spectra for different dopings. Uncertainties are derived from the one-sigma fit confidence intervals. Lines are linear fits to the data. (c) Slopes of the dispersions extracted from the linear fit in panel (b). The error bars in the slope are from the linear fit uncertainties. Red region indicates the doping where the antiferromagnetic Fermi surface reconstruction occurs. Red curve is a guide to the eye for the expected $\sqrt{x}$ dependence of the acoustic plasmon velocity at nonzero l. Red arrow highlights the plasmon velocity jump due to the carrier density change associated with the Fermi surface reconstruction (red shaded region). Insets in panel (c) show schematics of the Fermi surface with (left) and without (right) Fermi surface reconstruction in 1/4 of a Brillouin zone. Black dashed lines in the insets indicate the antiferromagnetic zone boundary. Blue color regions in panel (c) indicate the superconducting doping range. All spectra were taken using the photon energy at the peak of the x-ray absorption spectra (see extended Fig. 1) and at a temperature of 20 K.

summarized in Fig. 3(d). As can be seen, the charge excitation becomes dispersive at $h > 0.07$. Importantly, it appears to emerge from the dispersionless mode near the Brillouin zone center.

Figures 3(e)–3(g) shows the RIXS spectra taken with σ-polarized photons in a moderately doped sample ($x = 0.1$). Here, the magnon is much weaker and is not clearly observable in the spectra

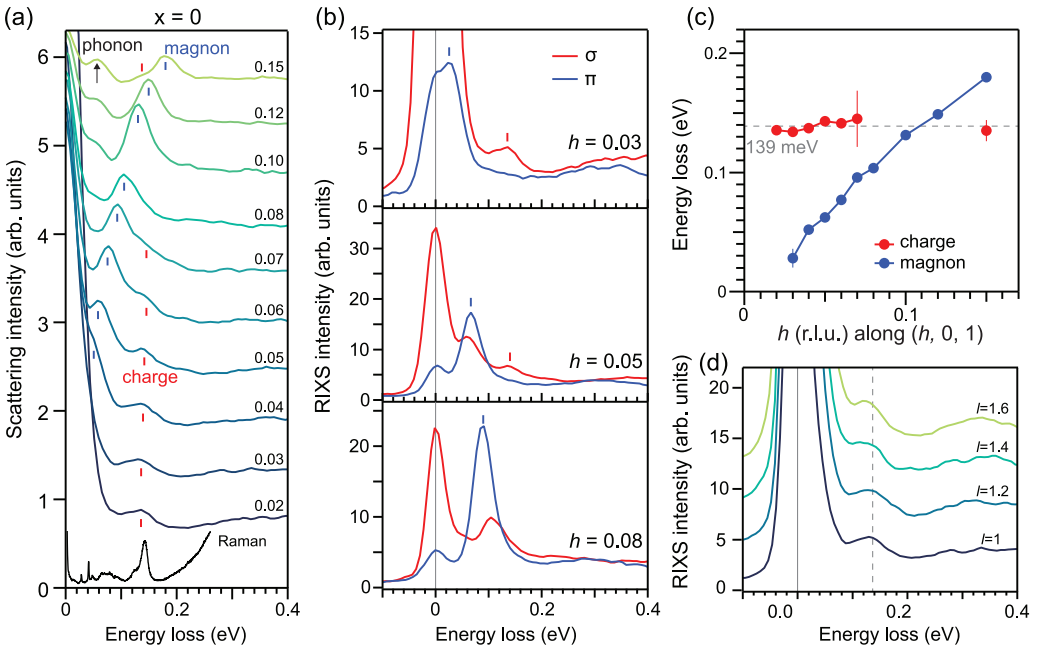


FIG. 2. Low-energy charge excitation in Nd_2CuO_4. (a) RIXS energy distribution curves along (h, 0, 1) for Nd_2CuO_4. Numbers next to each curve indicate the h value in r.l.u. Red markers indicate the charge excitation and blue markers highlight the magnon. Arrow pointing at a low-energy single-phonon peak around 50 meV. Note that this should not be interpreted as the single-phonon (Ω) mode associated with the 139 meV two-phonon (2Ω) excitation. Black curve at the bottom is the Raman spectroscopy data on Nd_2CuO_4. (b) RIXS curves at the indicated h value along (h, 0, 1), for σ and π photon polarizations. (c) Dispersion of the magnetic and charge excitations extracted from fits of the RIXS spectra. Vertical error bars are from the one-sigma fit confidence interval. (d) RIXS spectra along (0.03, 0, l), showing negligible dispersion in the out-of-plane l axis. Gray dashed lines in panels (c) and (d) indicate 139 meV.

taken with σ photons. Therefore, the dispersion of the charge excitations can be reliably extracted. As shown in Fig. 3(g), the collective charge excitations are well separated from the magnon dispersion, which is extracted from the spectra taken with π-polarized photons. Interestingly, the dispersionless region near the zone center is significantly reduced compared to the $x = 0.04$ sample. The dispersion anomaly manifests as a bend at low momenta near (0.02, 0, 1) with an energy scale of approximately 100 meV [Fig. 3(f)], representing further softening from 139 meV at zero doping and 120 meV at $x = 0.04$.

III. HYBRID LATTICE-PLASMON EXCITATION

The experimental observations here show that there is a complex evolution of the collective charge excitations between the undoped Mott insulator and the heavily doped metal. While the acoustic plasmons at high dopings are well understood, the nature of the charge excitations in the undoped and lightly doped regimes are unclear. The nondispersive mode observed in the undoped sample has an energy that is incompatible with the known phonons in the system [34]. There are also no features close to 139 meV in the optical conductivity of Nd_2CuO_4 [35]. However, this excitation energy can be associated with a lattice excitation involving two phonons, as there are single phonons with an energy near 70 meV [34]. This is consistent with observations in Raman scattering [36,37], where a peak at 1178 cm^{-1} (146 meV) was observed and attributed to two-phonon excitations arising from lattice anharmonicity. Alternatively, this mode could be understood as a local bound

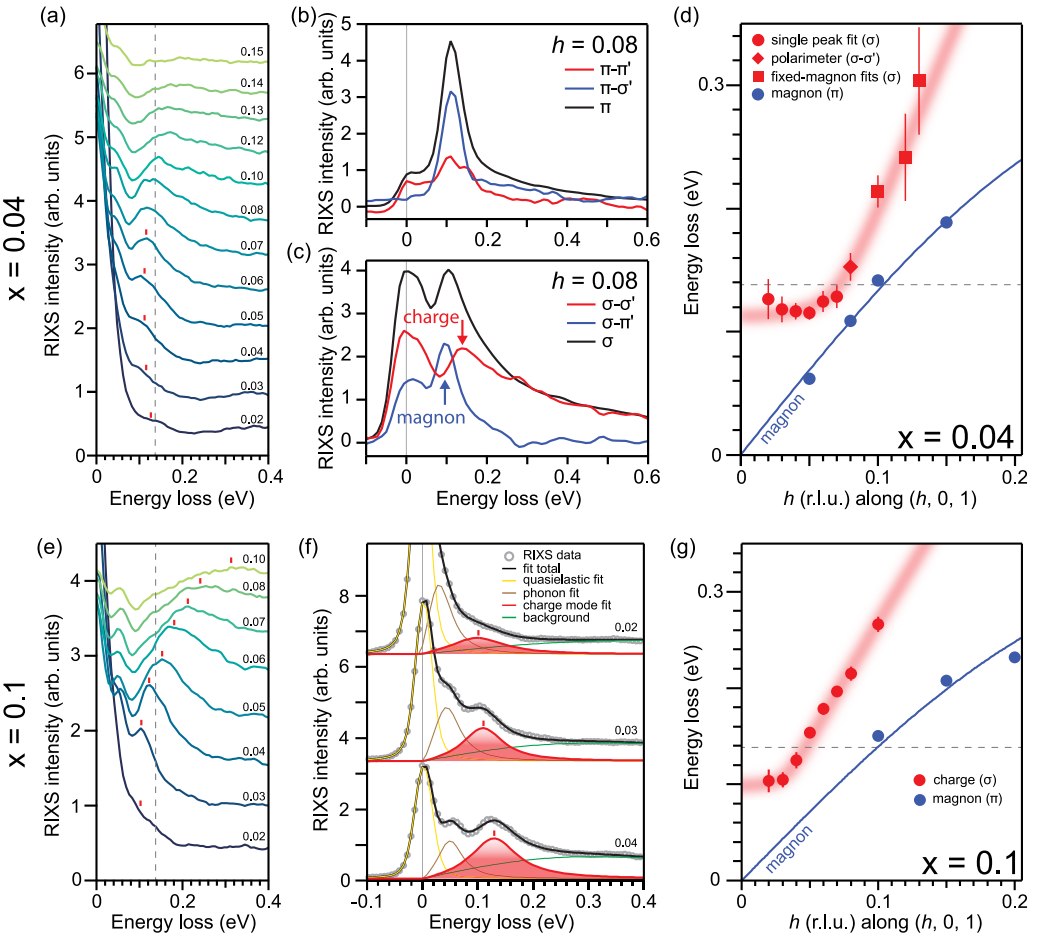


FIG. 3. Charge excitation dispersion anomalies in doped NCCO. (a) RIXS energy distribution curves along (h, 0, 1) for $Nd_{1.96}Ce_{0.04}CuO_4$. Polarization-resolved RIXS spectra at $h = 0.08$ for π incident photons [panel (b)] and σ incident photons [panel (c)]. Colored curves represent polarization-resolved spectra. Black curves represent spectra with integrated outgoing polarization. (d) Dispersions of excitations in the $x = 0.04$ sample (h, 0, 1) direction. The solid red circles, solid red diamonds, and solid red squares represent the charge excitation dispersion obtained using different analysis methods (see main text and extended data Fig. 3). Solid blue circles represent the magnon dispersion. (e) RIXS energy distribution curves for $Nd_{1.9}Ce_{0.1}CuO_4$. (f) Fitting for $x = 0.1$ spectra near the Brillouin zone center, with a quasielastic peak (yellow), a low-energy phonon (brown), a charge excitation (red), and a background that includes bimagnon and fluorescence features (green). (g) Dispersions of excitations in the $x = 0.1$ sample along the (h, 0, 1) direction. Numbers next to each curve in panels (a) and (e) indicate the momentum along (h, 0, 1); red markers indicate the charge excitation. Gray dashed lines in panels (a), (d), (e), and (g) indicate 139 meV. Solid blue lines in panels (d) and (g) are spin wave fits. Red shaded regions in panels (d) and (g) are guides to the eye for the hybrid charge excitation (see main text and Fig. 4). Vertical error bars are from the one-sigma fit confidence interval.

two-phonon excitation [38], which may be more consistent with the unusually high intensity of the observed mode. For generality, we use the term "2Ω excitation" to phenomenologically denote an excitation with twice the single-phonon energy, without distinguishing between the weakly coupled two-phonon overtone excitation and the strongly coupled bound biphonon. We also note that our Raman measurements reveal a shoulder feature at around 125 meV in addition to the main peak at around 140 meV [Fig. 2(a)], indicating that multiple 2Ω lattice excitations could be relevant.

Given the similar energy scales, the nondispersive mode in the RIXS spectra at zero doping is likely the same 2Ω excitation as observed in the previous Raman scattering results. We note that Raman scattering has also observed unusually intense 2Ω excitation in insulating *p*-type cuprates (La_2CuO_4, $YBa_2Cu_3O_{6.05}$, $Bi_2Sr_2YCu_2O_{8+\delta}$) at nearly the same energy as $Nd_{2-x}Ce_xCuO_4$ (NCCO) [39]. This supports the assignment of this 2Ω excitation to the same O motions within the CuO_2 plane, as the out-of-plane O are quite different between NCCO and the *p*-type parent compounds. Furthermore, La_2CuO_4 is close to being stoichiometric after annealing, unlike the other families. Thus, the observation of similar 2Ω excitations suggests that O defects likely do not play a significant role in the origin of this mode.

The observed dispersion anomaly in the lightly doped regime is consistent with coupling between the 2Ω excitation and the dispersive plasmon. The continuous doping-dependent energy shift of the RIXS zone center charge excitation and the same softening of the 2Ω mode observed independently by Raman spectroscopy (see Fig. S5 of the Supplemental Material [29]) further supports this picture. Figure 4(a) shows a homogeneous effective model that captures the eigenstates of a coupled lattice-plasmon hybrid mode. Here, the level repulsion between the hybridized branches of the lattice plasmon effectively opens a gap at the Brillouin zone center. In the RIXS measurements, the lower branch is difficult to observe within the experimental resolution due to the presence of additional single-phonon excitations and the elastic line broadening. Furthermore, if damping of the 2Ω excitation is strong, the lower branch can become broad and less visible than the upper branch (see Fig. S4 of the Supplemental Material [29]). We remark that the observed zone center gap in NCCO is unlikely associated with the plasmon gap induced by t_z interlayer hopping as proposed in some other cuprates [15]. Due to the lack of an apical oxygen and long inter-CuO_2 plane distance, the t_z in NCCO is expected to be the smallest among cuprates [40]. This is also supported by ARPES studies that report appreciable *c*-axis band dispersion in $La_{2-x}Sr_xCuO_4$ [41], but not in $Pr_{1.3-x}La_{0.7}Ce_xCuO_4$ [42] with the same crystal structure as NCCO.

Figures 4(b)–4(d) summarize the overall evolution of the collective charge excitations in the electron-doped cuprates. At half filling [Fig. 4(b)], the electron wave functions are localized to the Cu ions, and the only charge excitations below the charge transfer gap of about 1.5 eV [43] are single- and multiphonon excitations. With light doping, we expect that a small amount of spectral weight populates the Fermi level and acquire the potential to be mobile [44]. At low densities additional localizing interactions (e.g., Coulomb localization or disorder effects) can dominate [45], and in reality the low-temperature resistivity still behaves like an insulator at low dopings [46]. Thus, one does not expect the presence of propagating collective charge excitations in this regime, in stark contrast to our observation. However, it is well known that lightly doped cuprates tend to form nanoscale phase separation [47], which could naturally resolve this dilemma. In this view, the lightly doped system consists of regions with incipient metallicity that support plasmon-like charge fluctuations, coexisting with Mott-like regions where the 2Ω excitation is present [Fig. 4(c)]. Intraregion propagation is enabled by the plasmon component in the metallic regions, while coupling to the 2Ω excitation in the Mott regions both facilitates interregion propagation and renormalizes the effective velocity of the mode. At high dopings, where the electron wave functions are delocalized, metallic regions dominate and the collective charge excitations behave like free plasmons [Fig. 4(d)]. At the same time, the spectral signature of the 2Ω mode disappears due to diminishing insulating regions.

We remark that in the inhomogeneous model, the resulting spectra are not a simple sum of the spectral weight of the insulating and metallic components. Rather, the 2Ω excitation and dispersive plasmon are coupled near the boundaries. To demonstrate that the inhomogeneous scenario aligns with the simplified homogeneous two-mode hybridization model discussed in Fig. 4(a), we develop an effective theory based on a random network model, as presented in the Supplemental Material [29]. Disorder and damping are taken into account, which affect the coupling quantitatively but do not alter its fundamental nature. In addition, we emphasize that disorder alone cannot naturally account for the correlated doping dependence of the Raman 2Ω feature and the zone-center plasmon excitation energies observed in RIXS. Instead, the proposed inhomogeneous mode-coupling framework provides the most natural and consistent explanation. Finally, while our framework primarily

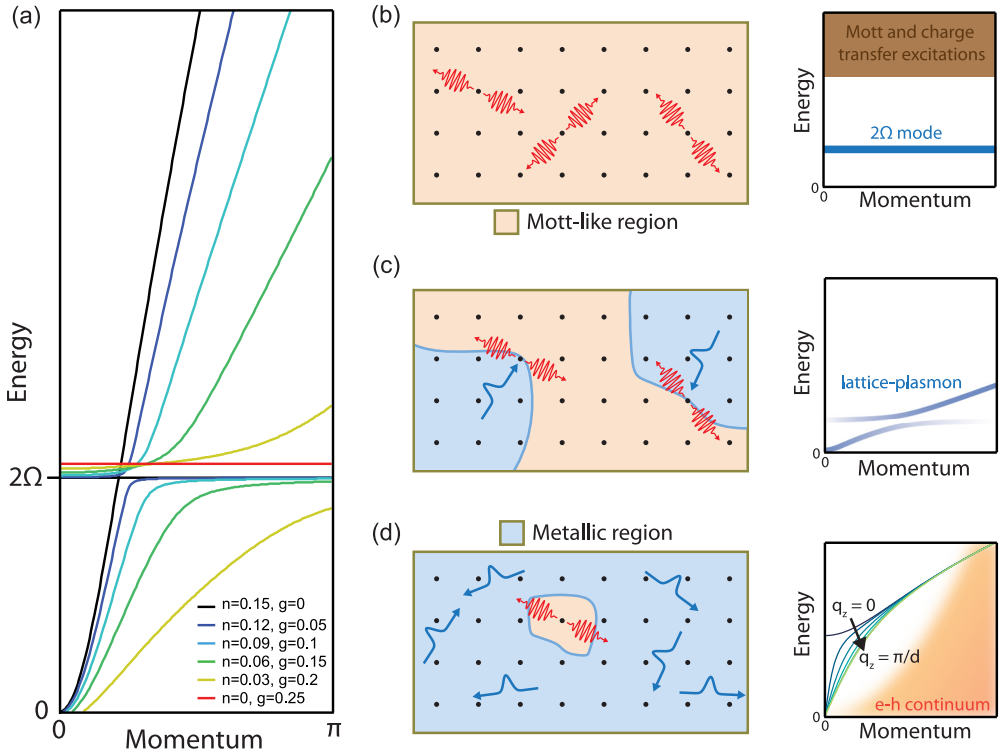


FIG. 4. (a) Schematic of a minimal, homogeneous effective model that captures—upon spatial averaging—the hybridization between a plasmon mode and a nondispersive 2Ω lattice excitation (see the Sec. II for details). The plasmon velocity decreases with decreasing doping, reflecting the reduced volume fraction of metallic regions and the emergence of a nearly nondispersive 2Ω mode associated with the Mott insulating phase. In addition, hybridization between these modes leads to an avoided crossing. Here, n denotes the carrier density, g is the coupling constant, and 2Ω corresponds to twice the energy of the oxygen phonon mode responsible for the dispersion kink observed in ARPES. For simplicity, here we ignore the effects of antiferromagnetic Fermi surface reconstruction. (b) At half filling, one electron is localized on each Cu site by strong Coulomb interactions, producing a Mott insulating state. The low-energy charge response contains a nondispersive 2Ω lattice excitation (right panel). Not shown are single-phonon excitations at lower energy. (c) With light doping, the system may contain nanoscale metallic regions embedded in a Mott-like matrix. Short-range plasmonic fluctuations in the metallic regions couple to nearby 2Ω lattice excitations, producing a broadened hybrid response with mixed lattice and plasmonic character (right panel). (d) In heavily doped systems with abundant metallic carriers, the collective charge excitations evolve into acoustic plasmons. The dispersion as a function of out-of-plane momentum q_z is shown on the right. Here, panel (d) denotes the interlayer spacing between CuO_2 planes.

addresses the deeply underdoped regime, a key open question is whether this mechanism bears a deeper connection to the spatial inhomogeneity of the superconducting gap and pseudogap observed by scanning tunneling microscopy at higher doping concentrations [47,48].

IV. IMPLICATIONS FOR CUPRATE PHYSICS

Our demonstration of the 2Ω excitation and its evolution to a gapped dispersive collective charge excitation is unexpected and has important implications for the nature of the cuprate ground state. Previously, hybridization between plasmons and single-phonon modes has been observed in low-density electron systems coupled to strongly polarizing phonons, such as graphene on SiC [49].

Furthermore, coupling between plasmons and single phonons in the cuprate context was theoretically investigated [50–52] but not yet experimentally identified. However, in the weak coupling limit, two-phonon overtone excitations arise from a high-order process and are normally extremely weak compared to single-phonon excitations, unlike what is observed here. Remarkably, our Raman results also show that while the single-phonon peaks exhibit little change with doping, the 2Ω excitation intensity is drastically reduced with increasing doping (see Fig. S5 of the Supplemental Material [29]). Additional experimental and theoretical efforts are required to clarify the nature of this unusual 2Ω excitation and its doping evolution.

As the ground-state wave function incorporates the zero-point fluctuations of these collective modes, it is likely that they leave a measurable imprint on the unconventional phases in the cuprates, including strange metallicity and high-temperature superconductivity. The observation of a similar 2Ω excitation mode in *p*-type cuprates with Raman scattering [39] suggests that 2Ω excitations and possibly lattice plasmons are ubiquitous in all cuprate families. Signatures of the hybrid mode may be difficult to resolve in the *p*-type cuprates with RIXS due to the relatively weaker signal.

In the layered cuprates, even though phonons are thought not to be the progenitors of the pairing interaction, it is widely documented that they strongly interact with the electronic states [53,54] and may play a critical role in enhancing superconductivity [55]. In particular, anisotropic electron-phonon interactions are thought to be beneficial to d-wave superconductivity [56]. While the coupling between single phonons and electrons is extensively studied in the cuprate context [57,58], 2Ω excitations and the putative hybrid lattice-plasmon modes have had much less considerations. How these 2Ω lattice excitations and the associated hybrid excitations interact with the antiferromagnetism is still an open question, and further work is required to elucidate any role these excitations may play in pairing. Regardless of their microscopic mechanisms and relation to electronic pairing, our results here have demonstrated that 2Ω excitations and plasmons play an important role in shaping the electronic landscape in the layered cuprates.

ACKNOWLEDGMENTS

We thank S. A. Kivelson, R. Hackl, B. Moritz, and D. Jost for insightful discussions. We are also grateful to V. R. Rocha, Y. Lyu, and J. Analytis for checking the doping levels with energy dispersive spectroscopy. The work performed at Stanford and SLAC was supported by the U.S. Department of Energy (DOE), Office of Basic Energy Sciences, Division of Materials Sciences and Engineering, Contract No. DE-AC02-76SF00515. The work performed at the University of California, Berkeley and Lawrence Berkeley National Laboratory was funded by the U.S. Department of Energy, Office of Science, Office of Basic Energy Sciences, Materials Sciences and Engineering Division, Contract No. DE-AC02-05-CH11231 within the Quantum Materials Program (KC2202). This work made use of the facilities at Diamond Light Source beamline I21 under Proposal No. MM42608.

DATA AVAILABILITY

The raw data of the main figures have been made available at a Dryad repository [60].

[1] D. Pines and D. Bohm, A collective description of electron interactions: II. Collective vs individual particle aspects of the interactions, Phys. Rev. **85**, 338 (1952).

[2] S. Martin, A. T. Fiory, R. M. Fleming, L. F. Schneemeyer, and J. V. Waszczak, Normal-state transport properties of $Bi_{2+x}Sr_{2-y}CuO_{6+\delta}$ crystals, Phys. Rev. B **41**, 846(R) (1990).

[3] S.-D. Chen, M. Hashimoto, Y. He, D. Song, K.-J. Xu, J.-F. He, T. P. Devereaux, H. Eisaki, D.-H. Lu, J. Zaanen, and Z.-X. Shen, Incoherent strange metal sharply bounded by a critical doping in Bi2212, Science **366**, 1099 (2019).

[4] R. L. Greene, P. R. Mandal, N. R. Poniatowski, and T. Sarkar, The strange metal state of the electron-doped cuprates, Ann. Rev. Mod. Phys **11**, 213 (2020).
[5] M. Mitrano, A. A. Husain, S. Vig, A. Kogar, M. S. Rak, S. I. Rubeck, J. Schmalian, B. Uchoa, J. Schneeloch, R. Zhong, G. D. Gu, and P. Abbamonte, Anomalous density fluctuations in a strange metal, Proc. Natl. Acad. Sci. USA **115**, 5392 (2018).
[6] J. G. Bednorz and K. A. Möller, Possible high-T_c superconductivity in the Ba-La-Cu-O system, Z. Phys. B **64**, 189 (1986).
[7] B. Keimer, S. A. Kivelson, M. R. Norman, S. Uchida, and J. Zaanen, From quantum matter to high-temperature superconductivity in copper oxides, Nature (London) **518**, 179 (2015).
[8] S. Sachdev, *Colloquium*: Order and quantum phase transitions in the cuprate superconductors, Rev. Mod. Phys. **75**, 913 (2003).
[9] P. A. Lee, N. Nagaosa, and X.-G. Wen, Doping a Mott insulator: Physics of high-temperature superconductivity, Rev. Mod. Phys. **78**, 17 (2006).
[10] Y. Cao, V. Fatemi, A. Demir, S. Fang, S. L. Tomarken, J. Y. Luo, J. D. Sanchez-Yamagishi, K. Watanabe, T. Taniguchi, E. Kaxiras, R. C. Ashoori, and P. Jarillo-Herrero, Correlated insulator behaviour at half-filling in magic-angle graphene superlattices, Nature (London) **556**, 80 (2018).
[11] B. Vignolle, A. Carrington, R. A. Cooper, M. M. J. French, A. P. Mackenzie, C. Jaudet, D. Vignolles, C. Proust, and N. E. Hussey, Quantum oscillations in an overdoped high-T_c superconductor, Nature (London) **455**, 952 (2008).
[12] M. Platé, J. D. F. Mottershead, I. S. Elfimov, D. C. Peets, R. Liang, D. A. Bonn, W. N. Hardy, S. Chiuzbaian, M. Falub, M. Shi, L. Patthey, and A. Damascelli, Fermi surface and quasiparticle excitations of overdoped $Tl_2Ba_2CuO_{6+\delta}$, Phys. Rev. Lett. **95**, 077001 (2005).
[13] A. Damascelli, Z. Hussain, and Z.-X. Shen, Angle-resolved photoemission studies of the cuprate superconductors, Rev. Mod. Phys. **75**, 473 (2003).
[14] M. Hepting, L. Chaix, E. W. Huang, R. Fumagalli, Y. Y. Peng, B. Moritz, K. Kummer, N. B. Brookes, W. C. Lee, M. Hashimoto, T. Sarkar, J.-F. He, C. R. Rotundu, Y. S. Lee, R. L. Greene, L. Braicovich, G. Ghiringhelli, Z. X. Shen, T. P. Devereaux, and W. S. Lee, Three-dimensional collective charge excitations in electron-doped copper oxide superconductors, Nature (London) **563**, 374 (2018).
[15] M. Hepting, M. Bejas, A. Nag, H. Yamase, N. Coppola, D. Betto, C. Falter, M. García-Fernández, S. Agrestini, K.-J. Zhou, M. Minola, C. Sacco, L. Maritato, P. Orgiani, H. Wei, K. Shen, D. Schlom, A. Galdi, A. Greco, and B. Keimer, Gapped collective charge excitations and interlayer hopping in cuprate superconductors, Phys. Rev. Lett. **129**, 047001 (2022).
[16] A. Nag, M. Zhu, M. Bejas, J. Li, H. C. Robarts, H. Yamase, A. N. Petsch, D. Song, H. Eisaki, A. C. Walters, M. García-Fernández, A. Greco, S. M. Hayden, and K.-J. Zhou, Detection of acoustic plasmons in hole-doped lanthanum and bismuth cuprate superconductors using resonant inelastic x-ray scattering, Phys. Rev. Lett. **125**, 257002 (2020).
[17] A. Nag, L. Zinni, J. Choi, J. Li, S. Tu, A. C. Walters, S. Agrestini, S. M. Hayden, M. Bejas, Z. Lin, H. Yamase, K. Jin, M. García-Fernández, J. Fink, A. Greco, and K.-J. Zhou, Impact of electron correlations on two-particle charge response in electron- and hole-doped cuprates, Phys. Rev. Res. **6**, 043184 (2024).
[18] V. Z. Kresin and H. Morawitz, Layer plasmons and high-T_c superconductivity, Phys. Rev. B **37**, 7854 (1988).
[19] Y. Ishii and J. Ruvalds, Acoustic plasmons and cuprate superconductivity, Phys. Rev. B **48**, 3455 (1993).
[20] A. Bill, H. Morawitz, and V. Z. Kresin, Electronic collective modes and superconductivity in layered conductors, Phys. Rev. B **68**, 144519 (2003).
[21] V. J. Emery and S. A. Kivelson, Importance of phase fluctuations in superconductors with small superfluid density, Nature (London) **374**, 434 (1995).
[22] J. Lin, J. Yuan, K. Jin, Z. Yin, G. Li, K.-J. Zhou, X. Lu, M. Dantz, T. Schmitt, H. Ding, H. Guo, M. P. M. Dean, and X. Liu, Doping evolution of the charge excitations and electron correlations in electron-doped superconducting $La_{2-x}Ce_xCuO_4$, npj Quantum Mater. **5**, 4 (2020).
[23] M. Naito, S. Karimoto, and A. Tsukada, Epitaxy-stabilized *n*-type superconducting cuprates, Supercond. Sci. Technol. **15**, 1663 (2002).

[24] M. Hepting, T. D. Boyko, V. Zimmermann, M. Bejas, Y. E. Suyolcu, P. Puphal, R. J. Green, L. Zinni, J. Kim, D. Casa, *et al.*, Evolution of plasmon excitations across the phase diagram of the cuprate superconductor $La_{2-x}Sr_xCuO_4$, Phys. Rev. B **107**, 214516 (2023).

[25] Y. Krockenberger, J. Kurian, A. Winkler, A. Tsukada, M. Naito, and L. Alff, Superconductivity phase diagrams for the electron-doped cuprates $R_{2-x}Ce_xCuO_4$ (R = La, Pr, Nd, Sm, and Eu), Phys. Rev. B **77**, 060505(R) (2008).

[26] N. P. Armitage, P. Fournier, and R. L. Greene, Progress and perspectives on electron-doped cuprates, Rev. Mod. Phys. **82**, 2421 (2010).

[27] K.-J. Xu, Q. Guo, M. Hashimoto, Z.-X. Li, S.-D. Chen, J. He, Y. He, C. Li, M. H. Berntsen, C. R. Rotundu, Y. S. Lee, T. P. Devereaux, A. Rydh, D.-H. Lu, D.-H. Lee, O. Tjernberg, and Z.-X. Shen, Bogoliubov quasiparticle on the gossamer Fermi surface in electron-doped cuprates, Nat. Phys. **19**, 1834 (2023).

[28] K.-J. Xu, J. He, S.-D. Chen, Y. He, S. N. Abadi, C. R. Rotundu, Y. S. Lee, D.-H. Lu, Q. Guo, O. Tjernberg, T. P. Devereaux, D.-H. Lee, M. Hashimoto, and Z.-X. Shen, Anomalous normal-state gap in an electron-doped cuprate, Science **385**, 796 (2024).

[29] See Supplemental Material at http://link.aps.org/supplemental/10.1103/nbry-mk8w for details on the materials and methods, which includes Ref. [59].

[30] W. S. Lee, J. J. Lee, E. A. Nowadnick, S. Gerber, W. Tabis, S. W. Huang, V. N. Strocov, E. M. Motoyama, G. Yu, B. Moritz, H. Y. Huang, R. P. Wang, Y. B. Huang, W. B. Wu, C. T. Chen, D. J. Huang, M. Greven, T. Schmitt, Z. X. Shen, and T. P. Devereaux, Asymmetry of collective excitations in electron- and hole-doped cuprate superconductors, Nat. Phys. **10**, 883 (2014).

[31] S. Das Sarma and E. H. Hwang, Collective modes of the massless Dirac plasma, Phys. Rev. Lett. **102**, 206412 (2009).

[32] Y. Dagan, M. M. Qazilbash, C. P. Hill, V. N. Kulkarni, and R. L. Greene, Evidence for a quantum phase transition in $Pr_{2-x}Ce_xCuO_{4-\delta}$ from transport measurements, Phys. Rev. Lett. **92**, 167001 (2004).

[33] E. M. Motoyama, G. Yu, I. M. Vishik, O. P. Vajk, P. K. Mang, and M. Greven, Spin correlations in the electron-doped high-transition-temperature superconductor $Nd_{2-x}Ce_xCuO_{4\pm\delta}$, Nature (London) **445**, 186 (2007).

[34] M. Hofmann, D. Strauch, U. Schroder, and E. Rampf, Lattice dynamics and inelastic neutron and synchrotron scattering cross-sections in Nd_2CuO_4, J. Phys.: Condens. Matter **6**, 3669 (1994).

[35] Y. Onose, Y. Taguchi, K. Ishizaka, and Y. Tokura, Charge dynamics in underdoped $Nd_{2-x}Ce_xCuO_4$: Pseudogap and related phenomena, Phys. Rev. B **69**, 024504 (2004).

[36] S. Sugai, T. Kobayashi, and J. Akimitsu, Magnons and phonons in Nd_2CuO_4, Phys. Rev. B **40**, 2686(R) (1989).

[37] B. Moritz, S. Johnston, T. P. Devereaux, B. Muschler, W. Prestel, R. Hackl, M. Lambacher, A. Erb, S. Komiya, and Y. Ando, Investigation of particle-hole asymmetry in the cuprates via electronic Raman scattering, Phys. Rev. B **84**, 235114 (2011).

[38] M. H. Cohen and J. Ruvalds, Two-phonon bound states, Phys. Rev. Lett. **23**, 1378 (1969).

[39] N. Chelwani, A. Baum, T. Böhm, M. Opel, F. Venturini, L. Tassini, A. Erb, H. Berger, L. Forró, and R. Hackl, Magnetic excitations and amplitude fluctuations in insulating cuprates, Phys. Rev. B **97**, 024407 (2018).

[40] R. S. Markiewicz, S. Sahrakorpi, M. Lindroos, H. Lin, and A. Bansil, One-band tight-binding model parametrization of the high-T_c cuprates including the effect of k_z dispersion, Phys. Rev. B **72**, 054519 (2005).

[41] M. Horio, K. Hauser, Y. Sassa, Z. Mingazheva, D. Sutter, K. Kramer, A. Cook, E. Nocerino, O. K. Forslund, O. Tjernberg, *et al.*, Three-dimensional Fermi surface of overdoped La-based cuprates, Phys. Rev. Lett. **121**, 077004 (2018).

[42] M. Horio, K. P. Kramer, Q. Wang, A. Zaidan, K. von Arx, D. Sutter, C. E. Matt, Y. Sassa, N. C. Plumb, M. Shi, *et al.*, Oxide Fermi liquid universality revealed by electron spectroscopy, Phys. Rev. B **102**, 245153 (2020).

[43] S. L. Cooper, G. A. Thomas, A. J. Millis, P. E. Sulewski, J. Orenstein, D. H. Rapkine, S.-W. Cheong, and P. L. Trevor, Optical studies of gap, exchange, and hopping energies in the insulating cuprates, Phys. Rev. B **42**, 10785(R) (1990).

[44] K. M. Shen, F. Ronning, D. H. Lu, W. S. Lee, N. J. C. Ingle, W. Meevasana, F. Baumberger, A. Damascelli, N. P. Armitage, L. L. Miller, Y. Kohsaka, M. Azuma, M. Takano, H. Takagi, and Z.-X. Shen, Missing quasiparticles and the chemical potential puzzle in the doping evolution of the cuprate superconductors, Phys. Rev. Lett. **93**, 267002 (2004).

[45] P. W. Anderson, Absence of diffusion in certain random lattices, Phys. Rev. **109**, 1492 (1958).

[46] Y. Onose, Y. Taguchi, K. Ishizaka, and Y. Tokura, Doping dependence of pseudogap and related charge dynamics in $Nd_{2-x}Ce_xCuO_4$, Phys. Rev. Lett. **87**, 217001 (2001).

[47] O. Fischer, M. Kugler, I. Maggio-Aprile, C. Berthod, and C. Renner, Scanning tunneling spectroscopy of high-temperature superconductors, Rev. Mod. Phys. **79**, 353 (2007).

[48] F. C. Niestemski, S. Kunwar, S. Zhou, S. Li, H. Ding, Z. Wang, P. Dai, and V. Madhavan, A distinct bosonic mode in an electron-doped high-transition-temperature superconductor, Nature (London) **450**, 1058 (2007).

[49] R. J. Koch, T. Seyller, and J. A. Schaefer, Strong phonon-plasmon coupled modes in the graphene/silicon carbide heterosystem, Phys. Rev. B **82**, 201413(R) (2010).

[50] T. Bauer and C. Falter, Impact of dynamical screening on the phonon dynamics of metallic La_2CuO_4, Phys. Rev. B **80**, 094525 (2009).

[51] C. Falter and M. Klenner, Nonadiabatic and nonlocal electron-phonon interaction and phonon-plasmon mixing in the high-temperature superconductors, Phys. Rev. B **50**, 9426 (1994).

[52] C. Falter, M. Klenner, and G. A. Hoffmann, Phonon renormalization and c-axis phonon-plasmon mixing in La_2CuO_4, Phys. Rev. B **52**, 3702 (1995).

[53] A. Lanzara, P. V. Bogdanov, X. J. Zhou, S. A. Kellar, D. L. Feng, E. D. Lu, T. Yoshida, H. Eisaki, A. Fujimori, K. Kishio, J.-I. Shimoyama, T. Noda, S. Uchida, Z. Hussain, and Z.-X. Shen, Evidence for ubiquitous strong electron–phonon coupling in high-temperature superconductors, Nature (London) **412**, 510 (2001).

[54] S. R. Park, D. J. Song, C. S. Leem, C. Kim, C. Kim, B. J. Kim, and H. Eisaki, Angle-resolved photoemission spectroscopy of electron-doped cuprate superconductors: Isotropic electron-phonon coupling, Phys. Rev. Lett. **101**, 117006 (2008).

[55] Y. He, M. Hashimoto, D. Song, S.-D. Chen, J. He, I. M. Vishik, B. Moritz, D.-H. Lee, N. Nagaosa, J. Zaanen, T. P. Devereaux, Y. Yoshida, H. Eisaki, D. H. Lu, and Z.-X. Shen, Rapid change of superconductivity and electron-phonon coupling through critical doping in Bi-2212, Science **362**, 62 (2018).

[56] C. Honerkamp, H. C. Fu, and D.-H. Lee, Phonons and d-wave pairing in the two-dimensional Hubbard model, Phys. Rev. B **75**, 014503 (2007).

[57] T. Cuk, F. Baumberger, D. H. Lu, N. Ingle, X. J. Zhou, H. Eisaki, N. Kaneko, Z. Hussain, T. P. Devereaux, N. Nagaosa, and Z.-X. Shen, Coupling of the B_{1g} phonon to the antinodal electronic states of $Bi_2Sr_2Ca_{0.92}Y_{0.08}Cu_2O_{8+\delta}$, Phys. Rev. Lett. **93**, 117003 (2004).

[58] T. P. Devereaux, T. Cuk, Z.-X. Shen, and N. Nagaosa, Anisotropic electron-phonon interaction in the cuprates, Phys. Rev. Lett. **93**, 117004 (2004).

[59] O. Matsumoto, A. Tsukada, H. Yamamoto, T. Manabe, and M. Naito, Generic phase diagram of $Nd_{2-x}Ce_xCuO_4$, Physica C **470**, S101 (2010).

[60] K.-J. Xu, Data for "Anomalous doping evolution of collective charge excitations in an n-type cuprate", Dryad Repository, 2026, https://doi.org/10.5061/dryad.n02v6wxbm.